

Flux inversion modeling across scales: The Carbon Monitoring System Multiresolution Flux (CMS-MFlux)



K. Bowman^{1,2}, M. Thill¹, B. Byrne¹, J. Liu¹

¹ Jet Propulsion Laboratory, California Institute of Technology, United States,

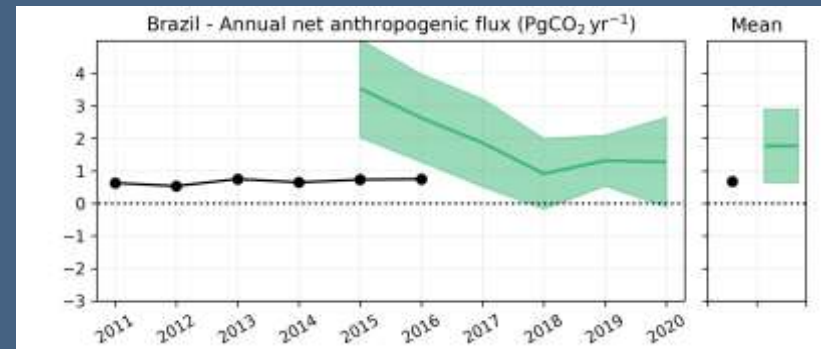
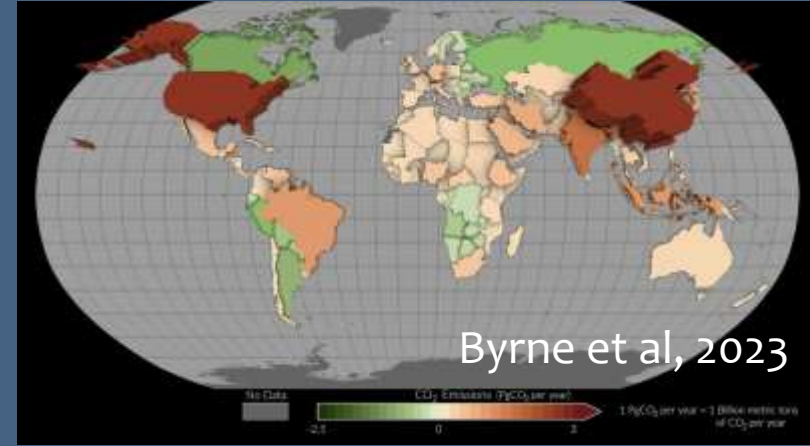
² Joint Institute for Regional Earth System Science and Engineering, University of California, Los Angeles, United States

Characterization of inversions: the problem of scale



The OCO-2 MIP and the CEOS Global Stocktake is a bellwether contribution to country-scale net emissions.

- What is the *flux resolution* of an inverse model estimate?
 - When and where do we have information?



What is resolution?

How do we quantify the ability to "resolve" one grid box relative to another?

A robust concept of resolution is well-developed in the remote sensing literature (Rodgers, 2000; Jones et al, 2003; Bowman et al, 2006, etc.)

$$\hat{\mathbf{x}} = \mathbf{x}_a + \mathbf{A}(\mathbf{x} - \mathbf{x}_a) + \epsilon$$

$$\frac{\partial \hat{\mathbf{x}}}{\partial \mathbf{x}} = \mathbf{A}$$

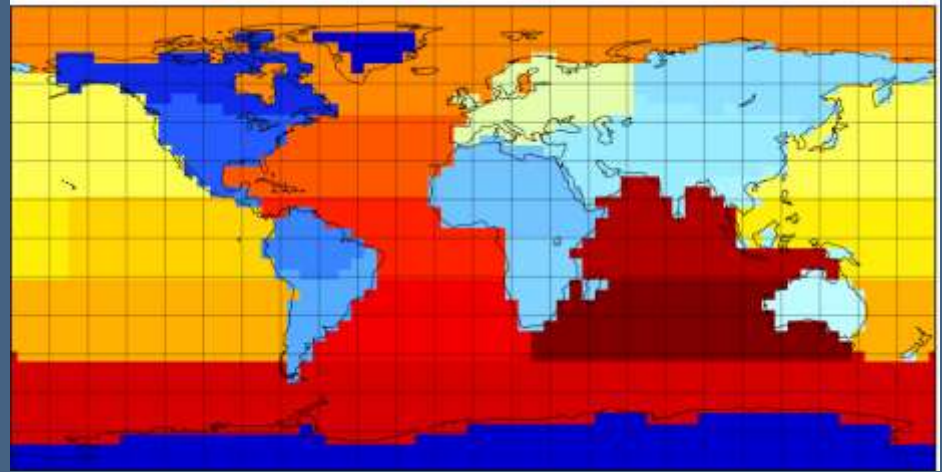
$$\text{dofs} = \text{Tr}(\mathbf{A})$$

4D-var and EnKF systems implicitly have an averaging kernel.

The problem is how to compute it.

The old standard TRANSCOM

- Inverse models minimize the Bayesian cost function.
- Analytic systems are explicit, but with a reduced control vector, \mathbf{z} .
 - Complete characterization, e.g., averaging kernels and diagnostics
- 4D-var systems are implicit, but with a full control vector, \mathbf{x} .
 - Approximate error characterization.



Guerne, 2002

$$J(\mathbf{x}) \equiv \frac{1}{2}(\underbrace{H\mathbf{x}}_{\text{forward model}} - \underbrace{\mathbf{y}}_{\text{data}})^T \underbrace{\mathbf{R}^{-1}}_{\text{model-data error covariance}} (\underbrace{H\mathbf{x}}_{\text{forward model}} - \underbrace{\mathbf{y}}_{\text{data}}) + \frac{1}{2}(\mathbf{x} - \underbrace{\mathbf{x}^b}_{\text{prior}})^T \underbrace{\mathbf{B}^{-1}}_{\text{prior error covariance}} (\mathbf{x} - \underbrace{\mathbf{x}^b}_{\text{prior}})$$

$$\mathbf{x}_a = \mathbf{x}_b + \mathbf{B}^{1/2}(\mathbf{I} + \mathbf{B}^{1/2}\mathbf{H}^T\mathbf{R}^{-1}\mathbf{H}\mathbf{B}^{1/2})^{-1}\mathbf{B}^{-1/2}\mathbf{H}^T\mathbf{R}^{-1}(\mathbf{y} - \mathbf{H}(\mathbf{x}))$$

Bridging the scales: a multiresolution approach

Start with a coarse basis set (e.g., TRANSCOM) and then build a set of *orthogonal* anomalies

$$f(x, y) = \sum_i \alpha_i \Phi_i(x, y) + \sum_j \gamma_j \Psi(x, y)$$

TRANSCOM

<<Ondelletes>>

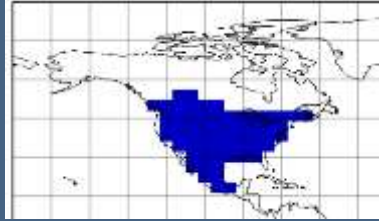
We can write this in vector-matrix format as This decomposition is *orthogonal*

$$\mathbf{x} = \mathbf{W}\mathbf{z}$$

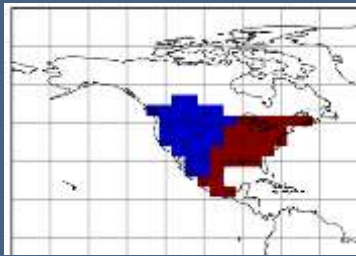
$$\mathbf{W}^\top \mathbf{W} = \mathbf{I}$$

First Multiresolution Refinement

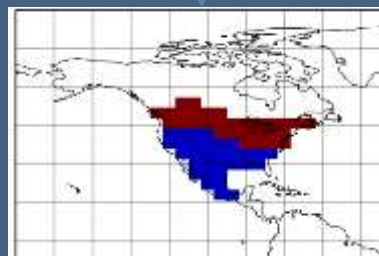
$$\Phi_{i,NA}$$



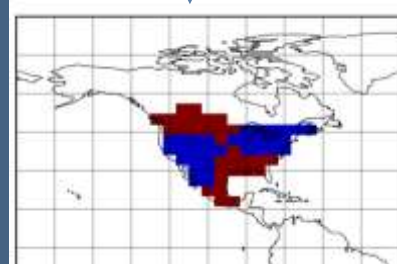
US is decomposed into a North-South, East-West, and Diagonal anomaly. These anomalies are orthogonal to each other and the North American mean flux



$$\Psi_{1,NA}$$

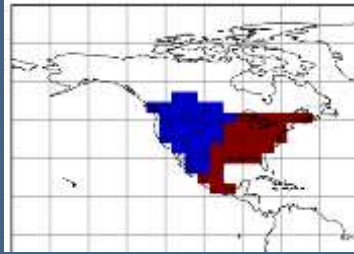


$$\Psi_{2,NA}$$



$$\Psi_{3,NA}$$

Second multiresolution refinement

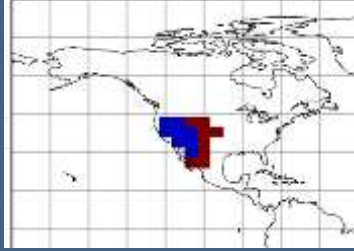


$$\Psi_{1,NA}$$

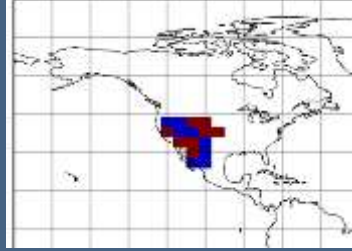
Successive refinements lead to a complete basis set for all grids. Each refinement is orthogonal to each other and upper/lower levels.



$$\Psi_{1,1,NA}$$



$$\Psi_{1,2,NA}$$



$$\Psi_{1,3,NA}$$

Emulation of CMS-Flux with CMS-MFlux

- An analytic solution requires a limited basis set-- $M \ll N$ wavelets.
- Here, we choose the wavelets that best represent the “support” of CMS-Flux

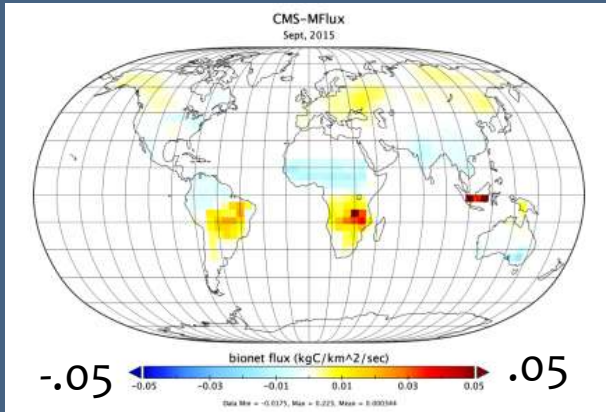
Choose ϕ_i for
$$\mathbf{x}_M = \sum_{i=1}^M \langle \mathbf{x}_{CMS}, \phi_i \rangle \phi_i$$

For this case, $M \sim 4000$, where $N \sim 40000$ for one year.
So, about 10% of all available grid boxes.

Adding the scales

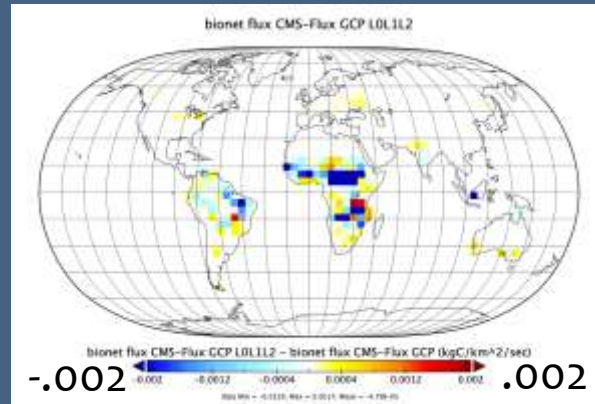
Adding more wavelets enables finer spatial resolution estimates.
Example of fluxes for Sept 2015

CMS-MFlux (all)



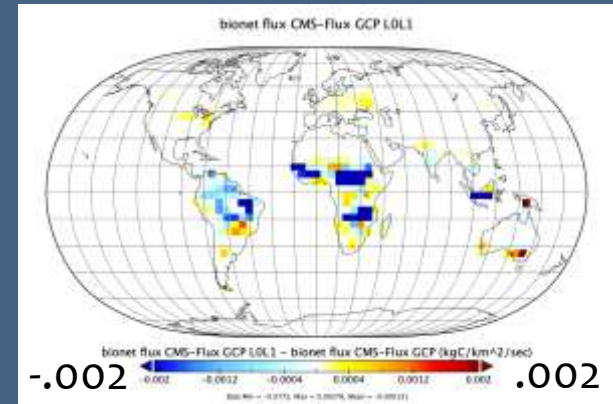
CMS-MFlux (all the scales)
(~325 wavelets)

all- Lo→L2



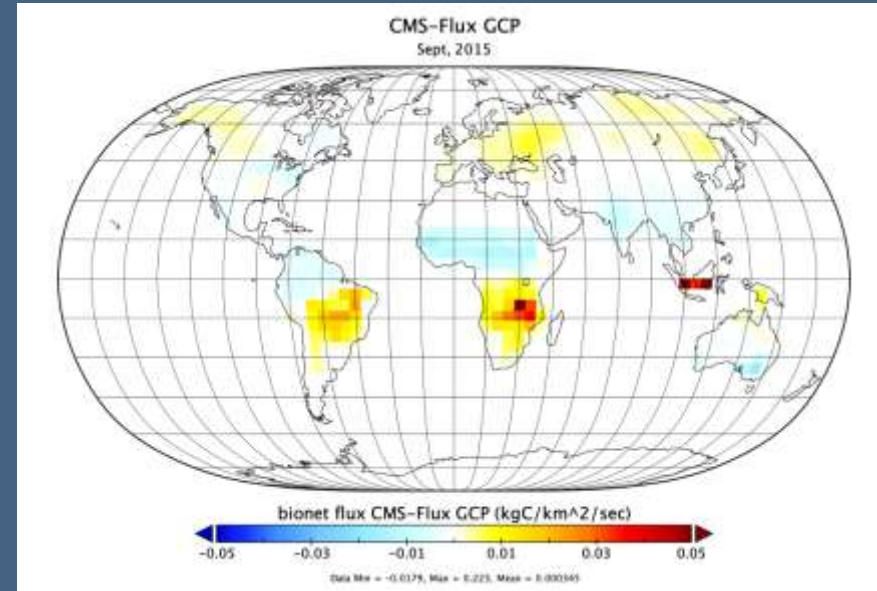
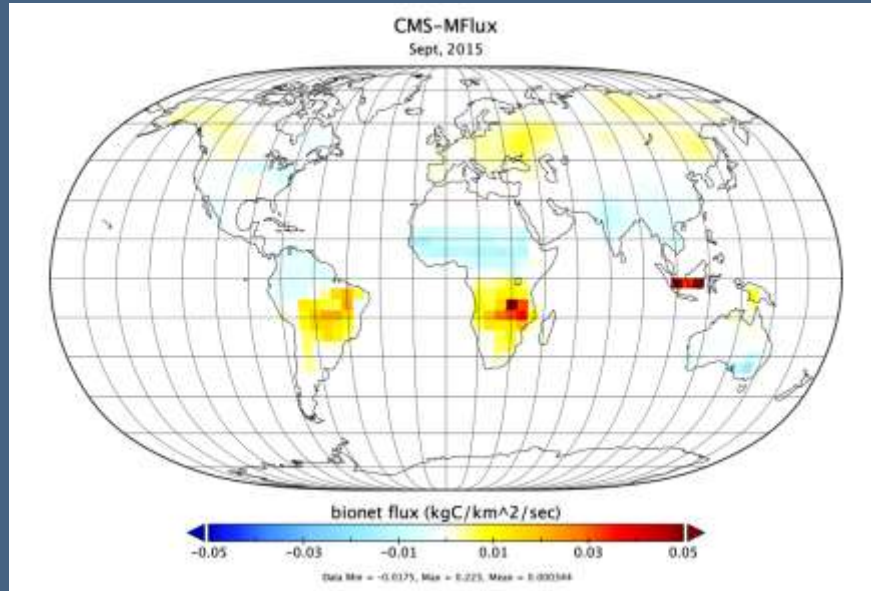
CMS-MFlux - Lo+L1+L2
(~135 wavelets)

all- Lo→L1



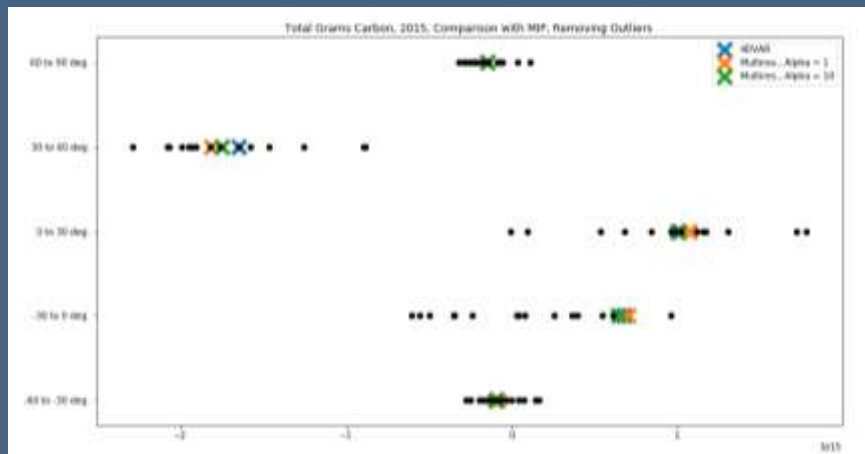
CMS-MFlux - Lo+L1
(~53 wavelets)

Comparison between CMS-Flux 4D-var and CMS-MFlux

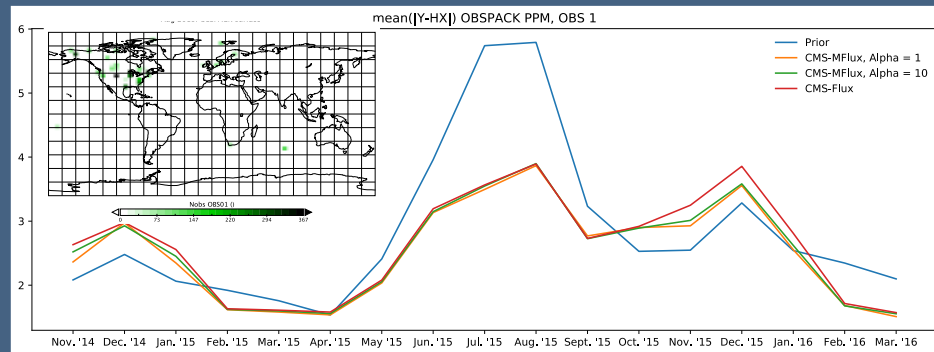


- CMS-Flux and CMS-Mflux use the same assimilation window and priors.
- CMS-MFlux basis and covariance are constructed to mimic the 4D-var solution.
 - Virtually the same flux pattern.

Comparison of CMS-MFlux to OBSPACK and OCO₂-MIP

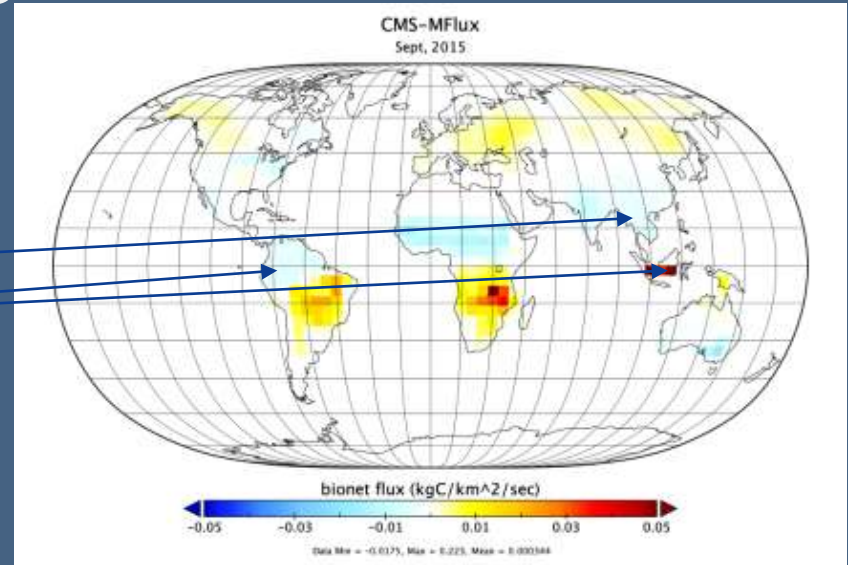
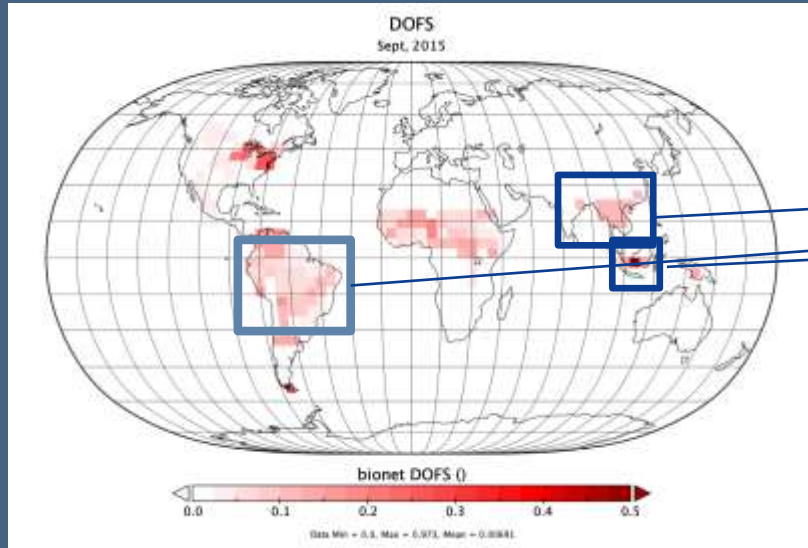


- CMS-MFlux is well within the range of the OCO₂-MIP ensemble
- CMS-MFlux and CMS-Flux are in close agreement



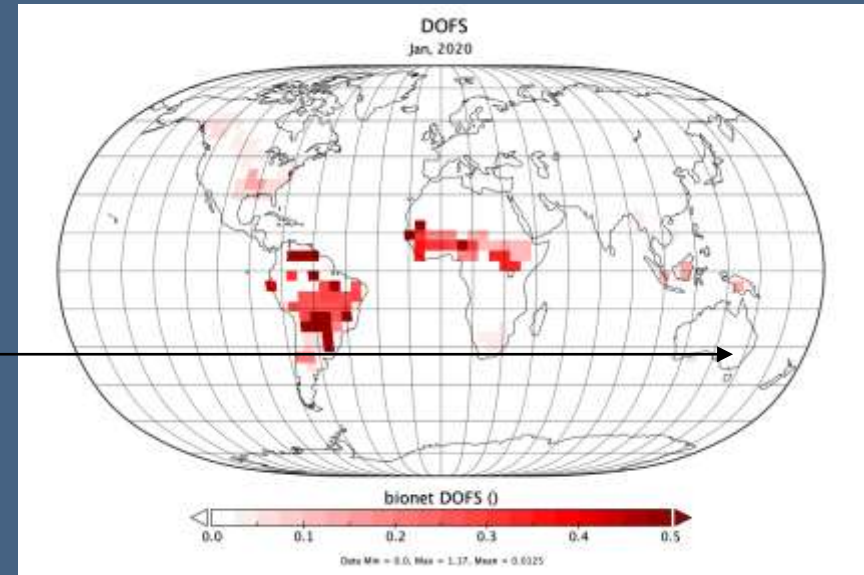
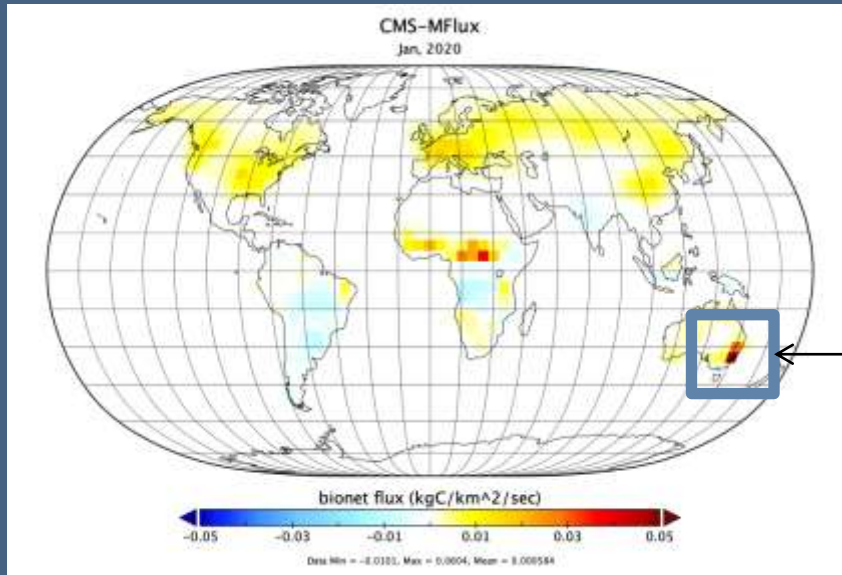
- CMS-MFlux is in substantially better agreement to independent observations (OBSPACK) relative to the prior
- Overall good agreement in errors between CMS-Flux and CMS-MFlux

Interpreting the inversion: Averaging Kernel



- Information content from OCO-2 for 2015
 - DOFS L0 = 33, L1 = 69, L2 = 134, total DOFS = 675
- Remarkably, Indonesia (Kalamantin) is resolvable in Sept. 2015.
- The dofs indicates that there is information in South America, Northern Africa, and Southeast Asia
- However, there is not information in Southern Africa

The inferno of 2020



- Australia suffered one of its worse biomass burning episodes in recent history.
- However, OCO-2 does not provide a strong constraint in Southeast Australia.

Some subtleties with DOFS calculation—the prior projection

- By approximating the solution \mathbf{x}_a of any χ^2 -minimizing inversion (e.g. 4D-var) in our wavelet basis, we can
 - simulate the inversion in the reduced-dimensional basis,
 - bound the associated DOFS with high probability.

$$\text{Tr} \left((\mathbf{C} + \Pi_{\mathbf{M}^T \tilde{\mathbf{x}}}^\perp \mathbf{M}^T \mathbf{B}^{-1} \mathbf{M} \Pi_{\mathbf{M}^T \tilde{\mathbf{x}}}^\perp + \mathbf{Y})^{-1} \mathbf{Y} \right) \lesssim \text{Tr}(\mathbf{A}) \lesssim \text{Tr} \left((\lambda \cdot \mathbf{M}^T \tilde{\mathbf{y}} \tilde{\mathbf{y}}^T \mathbf{M} + \mathbf{Y})^{-1} \mathbf{Y} \right)$$

DOFS of 4D-var

- If we use this as the prior covariance in the reduced-dimensional space, the corresponding low-dimensional inversion retrieves the 4D-var solution with negligible error.
- The posterior covariance and averaging kernel can then be computed analytically, and yield provable bounds on the corresponding quantities for the full-dimensional 4D-var system.

$$\begin{aligned} \mathbf{A} &:= (\mathbf{B}^{-1} + \mathbf{H}^T \mathbf{R}^{-1} \mathbf{H})^{-1} \mathbf{H}^T \mathbf{R}^{-1} \mathbf{H}, \text{ (the 4D-var averaging kernel)} \\ \mathbf{M} &:= \text{Matrix of columnized basis elements for reduced-dimensional space} \\ \tilde{\mathbf{x}} &:= \mathbf{x}_a - \mathbf{x}_b \\ \tilde{\mathbf{y}} &:= \mathbf{H}^T \mathbf{R}^{-1} (\mathbf{y} - H(\mathbf{x}_b) - \mathbf{H} \mathbf{M} \mathbf{M}^T \tilde{\mathbf{x}}) \\ \lambda &:= \frac{1}{\tilde{\mathbf{y}}^T \mathbf{M} \mathbf{M}^T \tilde{\mathbf{x}}} \\ \mathbf{Y} &:= \mathbf{M}^T \mathbf{H}^T \mathbf{R}^{-1} \mathbf{H} \mathbf{M} \\ \Pi_{\mathbf{M}^T \tilde{\mathbf{x}}} &:= \text{Projection onto } \mathbf{M}^T \tilde{\mathbf{x}} \\ \Pi_{\mathbf{M}^T \tilde{\mathbf{x}}}^\perp &:= \text{Projection onto the orthogonal complement of } \mathbf{M}^T \tilde{\mathbf{x}} \\ \mathbf{C} &:= \lambda \cdot [\Pi_{\mathbf{M}^T \tilde{\mathbf{x}}} \mathbf{M}^T \tilde{\mathbf{y}} \tilde{\mathbf{y}}^T \mathbf{M} \Pi_{\mathbf{M}^T \tilde{\mathbf{x}}} + \Pi_{\mathbf{M}^T \tilde{\mathbf{x}}}^\perp \mathbf{M}^T \tilde{\mathbf{y}} \tilde{\mathbf{y}}^T \mathbf{M} \Pi_{\mathbf{M}^T \tilde{\mathbf{x}}}^\perp + \Pi_{\mathbf{M}^T \tilde{\mathbf{x}}} \mathbf{M}^T \tilde{\mathbf{y}} \tilde{\mathbf{y}}^T \mathbf{M} \Pi_{\mathbf{M}^T \tilde{\mathbf{x}}}^\perp + \Pi_{\mathbf{M}^T \tilde{\mathbf{x}}}^\perp \mathbf{M}^T \tilde{\mathbf{y}} \tilde{\mathbf{y}}^T \mathbf{M} \Pi_{\mathbf{M}^T \tilde{\mathbf{x}}}^\perp] \end{aligned}$$

Conclusions

- Resolution and information content are critical metrics for inverse models and their use, e.g., Global Stocktake.
 - OCO-2 MIP ensembles are crude proxies for resolution
- CMS-MFlux shows that flux resolution—as defined by dofs--enabled by OCO-2 varies substantially in space and time in 4D-var systems.
 - Kalamantin was resolved in Sept, 2015, but not SE Australia in Jan 2020
 - Amazon and north-equatorial Africa can be inferred.
- For 2015, the dofs ~ 675, (~1.5% of all flux grids)
- CMS-MFlux can help interpret the OCO-2 MIP ensemble
 - Currently calculated for 2015-2020 in LNLGOIS